J. Membrane Biol. 176, 31–40 (2000)
DOI: 10.1007/s00232001073

The Journal of
Membrane
Biology

Muscarinic Activation of BK Channels Induces Membrane Oscillations in Glioma Cells and Leads to Inhibition of Cell Migration

A. Bordey[1], **H. Sontheimer**[1], **J. Trouslard**[2]
[1]Department of Neurobiology, University of Alabama at Birmingham, Birmingham, AL 35294 USA
[2]Institut de Physiologie URA 7519, 21 rue R. Descartes, 67084 Strasbourg Cedex France

Received: 17 December/Revised: 17 March 2000

Abstract. Patients with cerebral tumors often present with elevated levels of acetylcholine (ACh) in their cerebrospinal fluid. This motivated us to investigate physiological effects of ACh on cultured human astrocytoma cells (U373) using a combination of videomicroscopy, calcium microspectrofluorimetry and perforated patch-clamp recording. Astrocytoma cells exhibited the typical morphological changes associated with cell migration; polarized cells displayed prominent lamellipodia and associated membrane ruffling at the anterior of the cell, and a long tail region that periodically contracted into the cell body as the cell moved forward. Bath application of the ACh receptor agonist, muscarine, reversibly inhibited cell migration. In conjunction with this inhibition, ACh induced a dose-dependent, biphasic increase in resting intracellular free calcium concentration ($[Ca^{2+}]_i$) associated with periodic Ca^{2+} oscillations during prolonged ACh applications. The early transient rise in $[Ca^{2+}]_i$ was abolished by ionomycin and thapsigargin but was insensitive to caffeine and ryanodine while the plateau phase was strictly dependent on external calcium. The Ca^{2+} response to ACh was mimicked by muscarine and abolished by the muscarinic antagonists, atropine or 4-DAMP, but not by pirenzepine. Using perforated patch-clamp recordings combined with fluorescent imaging, we demonstrated that ACh-induced $[Ca^{2+}]_i$ oscillations triggered membrane voltage oscillations that were due to the activation of voltage-dependent, Ca^{2+}-sensitive K^+ currents. These K^+ currents were blocked by intracellular injection of EGTA, or by extracellular application of TEA, quinine, or charybdotoxin, but not by apamin. These studies suggest that activation of muscarinic receptors on glioma cells induce the release of Ca^{2+} from intracellular stores which in turn activate Ca^{2+}-dependent (BK-type) K^+ channels. Furthermore, this effect was associated with inhibition of cell migration, suggesting an interaction of this pathway with glioma cell migration.

Key words: BK channels — Muscarine — Acetylcholine — Calcium — Migration — Tumor

Introduction

Primary brain tumors (gliomas) derive from glial cells through an unknown malignant transformation. Glioma cells have the remarkable ability to migrate over long distances through the CNS and readily invade healthy brain tissue. The propensity of these cells to rapidly spread in the CNS has made it essentially impossible to surgically manage most gliomas. Glioma cell migration is poorly understood but is believed to involve changes in the interaction of glioma cells with extracellular matrix and also rearrangements in the cell cytoskeleton. This process is associated with upregulation of certain membrane receptors, such as platelet-derived growth factor (PDGF) and epidermal growth factor (EGF) receptors (Feldkamp, Lau & Guha, 1997; Guha, 1998; Shapiro & Shapiro, 1998). In addition, glioma cells are responsive to numerous neuropeptides and neurotransmitters, including, GABA, muscarine, histamine, NMDA, catecholamine, substance P and bradykinin (Brismar, 1995). Interestingly, cerebrospinal fluid (CSF) samples of patients with brain tumors show a significant increase in the content of acetylcholine (ACh) (Bychkovskii et al., 1998). ACh appears to be a potent mitogen for astrocytoma cells (Guizetti et al., 1997), suggesting that ACh receptor activation may participate in the malignant progression of glioma cells. Indeed, Aria-Montano et al.

Correspondence to: H. Sontheimer

(1994) showed expression of M3 muscarinic receptors in the astrocytoma cell line U373 whose activation by muscarine led to an increase in intracellular calcium and inositol-phosphate 3 (IP3). Little is known about the physiological effects of muscarinic receptor activation in glioma cells. In light of the overwhelming evidence suggesting an obligatory role for intracellular calcium fluctuations in cell migration (Marks & Maxfield, 1990; Rakic & Komuro, 1994; Gomez, Snow & Letourneau, 1995; Komuro & Rakic, 1996; Schwab et al., 1997), and the unusual propensity of glioma cells to migrate, we set out to investigate the physiological changes induced by muscarinic receptor activation and whether muscarinic receptor activation is coupled to cell migration. Using time-lapse video microscopy, we observed that muscarine reversibly inhibits migration of astrocytoma cells. This pathway involves release of calcium from thapsigargin-sensitive intracellular stores, which activates charybdotoxin-sensitive (BK-type) Ca^{2+}-dependent K^+ channels and leads to oscillations in the resting membrane potential.

Materials and Methods

Cell Culture

U373 MG cells were obtained from American Type Culture Collection (Rockville, MD). Cells were grown in a modified Eagle's minimum essential medium (MEM) supplemented with 10% fetal calf serum, 2 mM L-glutamine, 1 mM MEM vitamin, 1 mM sodium pyruvate, 1 mM nonessential amino acids, penicillin (50 U/ml) and streptomycin (50 μg/ml). Cells were kept in a humidified atmosphere (5% CO_2, 95% air) at 37°C. Confluent cells were rinsed with a calcium and magnesium-free Earle's Balanced Salt Solution (EBSS) and treated with trypsin solution (0.5 g/l) containing EDTA (ethylenedinitrilo)tetraacetic acid) (0.2 g/l). Cells were harvested by centrifugation at 800 rpm for 10 min and plated into a recording chamber. This chamber consisted of a glass ring (diameter, 16 mm; height, 3 mm) attached to a polyornithine-coated (Sigma) glass coverslip with Sylgard (Dow Corning). Experiments were performed on nonconfluent cells two to three days after plating.

Intracellular Calcium Measurements

Intracellular free calcium concentration was measured from indo-l fluorescence (Grynkiewicz, Poenic & Tsien, 1985). Cells were preloaded with the acetoxymethyl ester form of indo-1 (indo-l-AM; 2 μM) 1 hr in culture medium at 37°C. Cells were then superfused with the external solution for 30 min to allow for complete ester hydrolysis. The culture chamber was transferred onto the stage of an Olympus inverted microscope (IMT-2) fitted with epifluorescence illumination. UV excitation was provided by a Xenon arc lamp (Osram XBO-75, Germany) and a 360 nm excitation filter. UV light was reflected by a 380 nm dichroic mirror and transmitted to the cell by an oil immersion objective (Nikon fluorite 40×, NA 1.3). Emitted light was split by a 455 nm dichroic mirror to two photomultipliers (Hamamatsu type RI 104 supplied by a 700 volts DC voltage source) at 405 and 485 nm. Recordings were spatially restricted to a single cell by a rectangular diaphragm. Anodal currents of the photomultipliers were converted to voltage by home-built converters. The voltages were digitized using the labmaster TL-1 interface driven by home made software written in Axobasic (version 1.1). This software allowed online calculation of the emission ratio (R) of 405 nm/485 nm and converted the acquired ratio to calcium concentration using the equation: $[Ca^{2+}]_i = K_d \cdot (F_o/F_s) \cdot (R - R_{min})/(R_{max} - R)$ where R_{min} = minimum value of R at zero $[Ca^{2+}]$; R_{max} = value of R at saturating $[Ca^{2+}]$; K_d = dissociation constant of indo-l for calcium; F_o/F_s = maximum excursion at 485 nm. Signals were calibrated using increasing concentrations of $CaCl_2$ added to 140 mM KCl, 20 mM EGTA, 10 mM HEPES and 50 μM indo-l, pH 7.2. The theoretical value of free $[Ca^{2+}]_i$ was calculated using the program React (version 2.01) designed by G.L. Smith (Department of Physiology, University of Glasgow, UK). $(R - R_{min})/(R_{max} - R)$ was then plotted against the calculated $[Ca^{2+}]_i$ and the constant $K_d \cdot (F_o/F_s)$ determined by linear regression. The best fit was obtained using $R_{min} = 0.07$, $R_{max} = 2.5$ and $K_d \cdot (F_o/F_s) = 467$ nM. However, in vivo calibrations using patch-clamp techniques gave a higher R_{min} value (0.2) with no significant difference in R_{max} and $K_d \cdot (F_o/F_s)$ values. This value of 0.2 as R_{min} was therefore used. Indo-1 values were corrected for background fluorescence.

Time-Lapse Video Microscopy

Coverslips were placed on the stage of a LU-CB-1 tissue culture chamber (Medical Systems, Greenvale, NY) equipped with an NP-2 incubator (Nikon, Japan) to maintain temperature at 37°C and atmosphere at 95% O_2/5% CO_2. Cells were visualized using a Nikon Diaphot inverted microscope with phase contrast optics and a 20× objective. Images were captured on a time-lapse VHS video recorder/player and digitized offline using a frame grabber (Snappy). The medium containing muscarine (50 μM) was bath-applied after complete exchange of the control medium.

Electrophysiology

Patch-clamp recordings were made in the whole-cell (Hamill et al., 1981) and perforated patch (Rae et al., 1991) configurations using a List EPC7 patch amplifier. Electrodes were pulled from softglass haematocrite tubes on a vertical List puller (L/P-3P-A). The standard patch pipette solution had the following composition (mM): KCl, 140; $MgCl_2$, 1.2; HEPES, 10; pH adjusted to 7.2 with KOH. Electrodes had a resistance of 2 to 3 MΩ when filled with the above potassium-based solution. Whole-cell current and voltage commands were produced and digitized online by a Labmaster TLI interface driven by PClamp software (version 5.5). In some cases, the emission ratio of 405/480, the voltage and current were digitized using home-made software written in Axobasic.

Perforated Patch Clamp

We utilized the perforated patch method using amphotericin B. A freshly made stock solution of amphotericin B (3 mg/100 μl) was made in dimethylsulfoxide (DMSO) and ultrasonicated in pipette solution to a final concentration of 0.3 mg/ml. To improve gigaseal formation, tips of electrodes were dipped into pipette solution for 5–20 sec and then back-filled with the amphotericin-containing solution. After formation of the gigaseal, a low access resistance (5 to 10 MΩ) was typically obtained within 4 min.

Solutions and Drugs

The standard external solution had the following composition (mM): NaCl, 140; KCl, 3; $CaCl_2$, 2.5, $MgCl_2$, 1.2; glucose, 10; HEPES, 10, (pH adjusted to 7.2 with NaOH). A Ca^{2+}-free solution was made by replacing $CaCl_2$ with 5 mM $MgCl_2$ and adding 500 μM ethylene glycol bis-(β-aminoethyl ether)N,N,N′,N′tetraacetic acid (EGTA). During experiments, cells were continuously perfused with the extracellular solution (5–10 ml/min) in a recording chamber that holds 500 μl volume. Experiments were performed at room temperature (20–25°C).

ACh, muscarine, amphotericin B, atropine, quinine, ionomycin, thapsigargin (TG), caffeine, ryanodine and EGTA were obtained from Sigma Chemical (St. Louis, MO). Indo-l and indo-l-AM were from Molecular Probes (Eugene, OR). Apamin and charybdotoxin (ChTx) were from Latoxan. Pertussis toxin (PTX) was obtained from Biochem (France). D-IP3 was purchased from Alomone. Pirenzepine and 4-DAMP (4-diphenyl acetoxy-methyl piperidine methiodide) were a generous gift from Dr. M.P. Caufield (Department of Pharmacology, UCL, London, UK). Drugs were dissolved in extracellular medium and applied either by bath perfusion or by pressure ejection. When using pressure ejection, drugs were applied from a micropipette located 20 μM from the cell. TG and ionomycin were dissolved in DMSO. The final concentration of DMSO was 0.1%. In control experiments where DMSO was applied alone at this concentration it had no effect on $[Ca^{2+}]_i$. Results are expressed as mean ± SEM, with the number of cells (*n*) given between parentheses.

Results

Muscarinic Arrest of U373 Astrocytoma Cell Migration

Migration of U373 MG astrocytoma cells was studied by time-lapse video microscopy. Representative examples of migrating glioma cells are displayed in Fig. 1. Migrating cells displayed a polarized shape that often included a long tail at their posterior and prominent lamellipodia at their anterior ends. Migration was associated with cyclic morphological changes consisting of first elongation of the cell body and extension of lamellipodia, followed by retraction of the tail portion of the cell. The mean rate of migration was 16.8 ± 1.1 μm/hr (n = 10 cells). When contacting adjacent cells, motile cells often slowed and/or changed direction but continued migration. Application of muscarine (50 μM–100 μM) for 1–3 hr reversibly inhibited cell migration (Fig. 2, N = 3 experiments, n = 6 cells).

To further understand the physiological mechanism associated with the inhibition of cell migration we investigated the effect of focal ACh application on single cells while monitoring $[Ca^{2+}]_i$ and for some cells performed combined $[Ca^{2+}]_i$ measurements and patch-clamp recordings.

Calcium Fluctuations Induced by Acetylcholine

With 2.5 mM external Ca^{2+}, unstimulated cells displayed a $[Ca^{2+}]_i$ of 118 ± 3 nM (n = 64). Pressure application

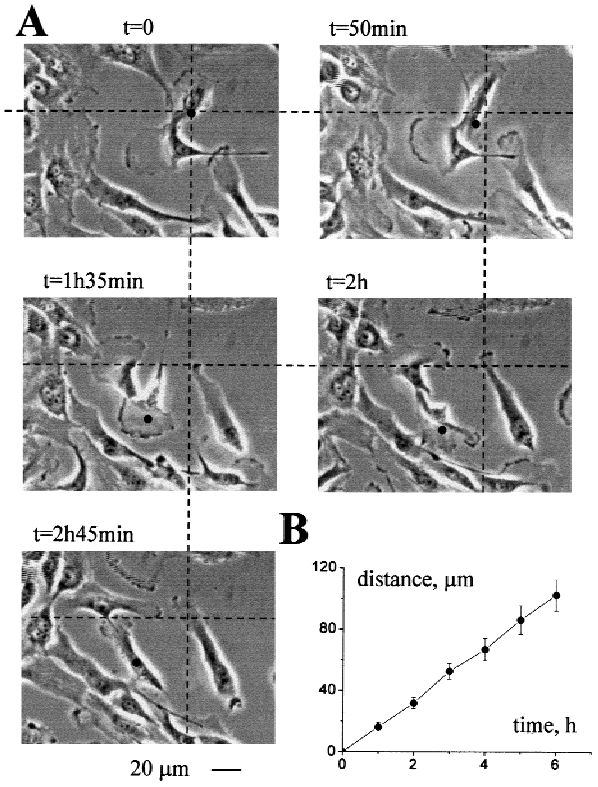

Fig. 1. Migration of U373 MG cells. (*A*) Pictures were taken every 5 min with representative examples shown at time zero, 50 min, 1 hr 35 min, 2 hr and 2 hr 45 min. The flat lamellipodium and the prominent cell body of the cell marked with a dot are clearly distinguishable. The dotted lines represent a spatial reference as the starting point of the cell migration. (*B*) Migration is plotted as a function of time with an average speed of 17.1 μm/hr (n = 10).

of ACh (50 μM) induced a biphasic increase in $[Ca^{2+}]_i$ which consisted of an initial peak followed by a longer lasting plateau. The duration of the plateau corresponded to the time of agonist application and could last for several minutes (Fig. 3*A*). Also, these repetitive applications of ACh resulted in a progressive decrease in the amplitude of the Ca^{2+} response (Fig. 3*A*). Prolonged applications of ACh (200 μM) often resulted in regenerative and regular calcium oscillations superimposed on the plateau phase (Fig. 3*A* and 5*A*, *B*). The effect of ACh on $[Ca^{2+}]_i$ was mimicked by muscarine (50 μM) and fully blocked by atropine (10 to 100 nM; Fig. 3*B*) and 4-DAMP (10 nM; Fig. 6*A*), but not by pirenzepine (10 nM to 10 μM; *data not shown*). The nicotinic receptor agonist, dimethylphenylpiperazinium (DMPP), had no effect on $[Ca^{2+}]_i$ (*data not shown*). The ACh-induced increase in $[Ca^{2+}]_i$ was dose-dependent with a threshold concentration of 0.3 μM, an EC_{50} of 1.3 μM, and a maximum response observed with concentrations above 3 μM (Fig. 3*C*). To determine whether PTX-sensitive G proteins mediate the ACh-induced increase of $[Ca^{2+}]_i$, dishes were pretreated for 24 hr with 500 ng/ml of PTX. PTX-

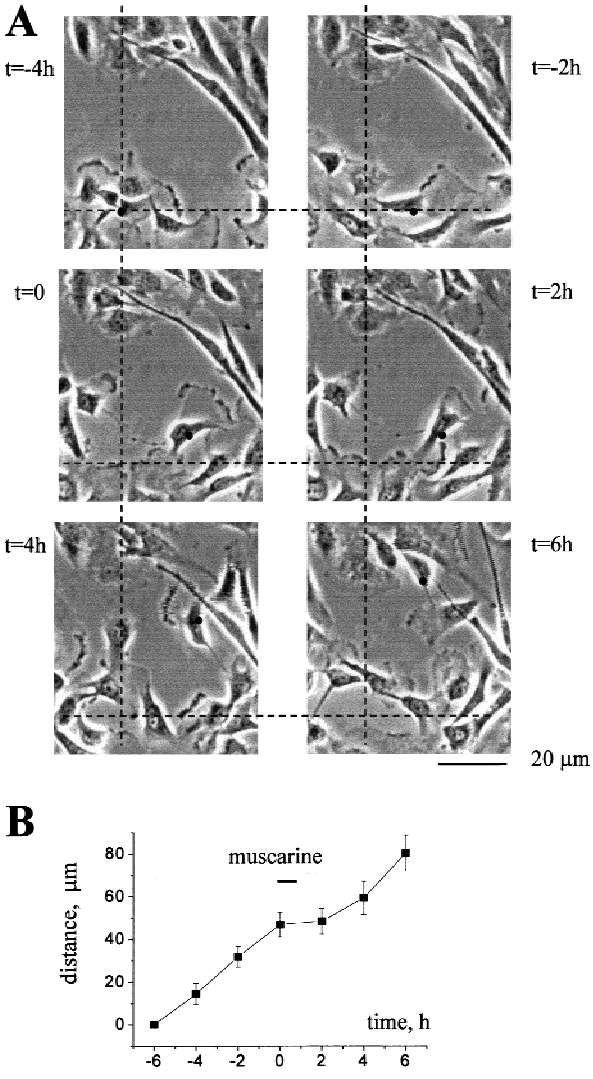

Fig. 2. Muscarine inhibits migration. (*A*) Effect of a muscarinic application (1 hr) on the migration of a representative cell (marked with a dot). The dotted lines represent a spatial reference as the starting point of the cell migration. (*B*) Migration of cells ($n = 6$) is plotted as a function of time. Muscarine, a muscarinic cholinergic receptor agonist (50 μM) reversibly inhibited the migration.

treated and control cells were separately loaded with indo-l-AM. The PTX pretreatment did not significantly alter either the presence of ACh-induced Ca^{2+} oscillations or the amplitude of the response (*data not shown*).

Calcium Sources

Intracellular Ca^{2+} increases can be due to an influx through the plasma membrane or release from intracellular stores. The mean resting Ca^{2+} concentration has been evaluated before and after substitution of external Ca^{2+} with Mg^{2+}/500 μM EGTA for 9 cells. For these cells, $[Ca^{2+}]_i$ was 124 ± 21 nM with 2.5 external calcium and 91 ± 10 nM with 0 external calcium. These values are not significantly different. However when comparing the values of $[Ca^{2+}]_i$ in cells recorded in a 0 external calcium (91 ± 2 nM ($n = 27$)) or in a 2.5 mM external calcium (*see* value above), these $[Ca^{2+}]_i$ values are significantly different ($P < 0.0001$). This suggests that an ongoing Ca^{2+} influx was present in these cells (Fig. 4*A*). Removal of external Ca^{2+} abolished the plateau phase of the ACh (30 μM)-induced $[Ca^{2+}]_i$ increase. Reintroduction of Ca^{2+} to the bath led to the rapid reappearance of a sustained Ca^{2+} rise. This suggests the biphasic response is due to an initial Ca^{2+} release from intracellular stores followed by Ca^{2+} influx across the membrane.

To evaluate the participation of internal Ca^{2+} stores in the ACh-induced $[Ca^{2+}]_i$ rise, reagents known to deplete internal Ca^{2+} stores, including ionomycin, caffeine, ryanodine and thapsigargin (TG) were applied to the cells. The first application of ionomycin (1 μM) induced a large increase in $[Ca^{2+}]_i$ of 1286 ± 284 nM ($n = 14$) and reversibly suppressed the ACh-induced $[Ca^{2+}]_i$ increase (Fig. 4*B*). Since the depletion of internal stores by ionomycin blocked the ACh response, we then used more selective agents. Specifically, we applied caffeine and ryanodine to interfere with caffeine and/or ryanodine-sensitive Ca^{2+} stores, and TG to deplete IP3-sensitive Ca^{2+} stores. In all experimental cells, caffeine (10 mM, $n = 10$) and ryanodine (10 μM, $n = 5$) had no effect on $[Ca^{2+}]_i$. In the presence of 2.5 mM extracellular Ca^{2+}, TG (1 μM) applied for 1 sec increased $[Ca^{2+}]_i$ to 291 ± 44 nM ($n = 12$) for over 30 min (*data not shown*). In absence of external calcium, the $[Ca^{2+}]_i$ increase induced by thapsigargin was transient (Fig. 4*C*, inset) and peaked at 350 ± 59 nM ($n = 5$) before returning to basal levels. Reintroduction of external Ca^{2+} immediately resulted in the appearance of sustained calcium increase. In Fig. 4*C*, TG progressively reduced the ACh (200 μM)-evoked $[Ca^{2+}]_i$ increase until a total and irreversible inhibition was achieved. This suggests that the initial ACh-induced Ca^{2+} elevation was a result of release from IP3-sensitive stores.

Muscarine-induced BK Channel Activation and Membrane Oscillations

Biophysical properties of Indo-l loaded U373 cells were assayed using the perforated patch-clamp technique. Under current-clamp conditions, cells had a resting potential of −27 ± 2 mV ($n = 30$), an input resistance of 297 ± 79 MΩ ($n = 15$) and a membrane capacitance of 110 ± 10 pF ($n = 17$). Brief application of ACh (200 μM) induced a hyperpolarization to −53 ± 9 mV ($n = 6$) from the resting potential (*data not shown*). Under volt-

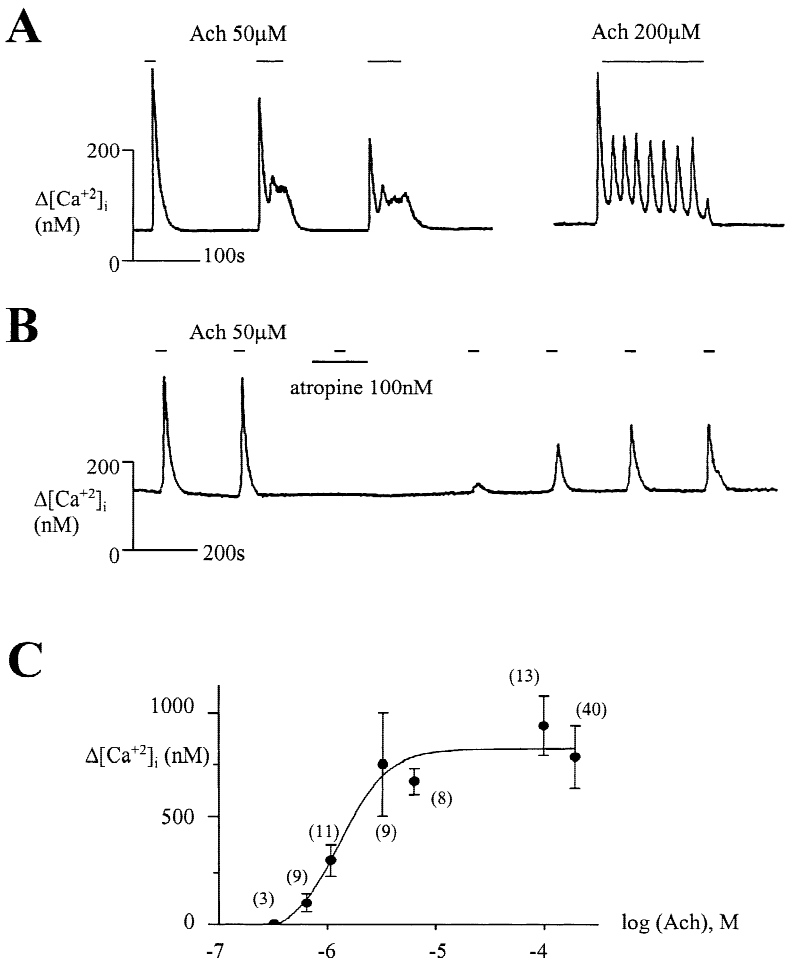

Fig. 3. Muscarinic receptor activation induces Ca^{2+} increase (ΔCa). (*A*) Left trace represents the effect of acetylcholine (ACh, 50 μM) applied by pressure during the time indicated by the bars. In the cell illustrated on the right, 200 μM ACh applied by pressure for 3 min induced regenerative calcium oscillations. (*B*) Atropine (100 nM) bath applied during the time indicated by the bar reversibly inhibited the $[Ca^{2+}]_i$ induced by ACh (50 μM). ACh was applied by pressure for 10 sec every 3 min. (*C*) Relationship between the increase in internal free calcium concentration (ΔCa) and the concentration of ACh. Data are means ± SEM and *n*, the number of cells tested, is given for each concentration.

age-clamp at −20 mV, ACh (20 μM) induced an outward current of 741 ± 143 pA ($n = 32$) and an increase in calcium of 538 ± 33 nM ($n = 25$). Prolonged application of ACh (200 μM) induced Ca^{2+} oscillations (Fig. 5*Aa* and *Ba*) that were in phase with holding current (Fig. 5*Ab*) or membrane potential (Fig. 5*Bb*) oscillations. Close examination of recordings showed that the Ca^{2+} rise always preceded the development of the outward current (dashed lines). A $[Ca^{2+}]_i$ threshold of 120 nM was required to activate the current. The reversal potential was determined by using a voltage ramp protocol (from −120 to +160 mV) applied at the peak of the ACh-induced outward current (Fig. 5*C*, left panel). With 3 mM external K^+, the reversal potential of the ACh-induced current (E_{rev}) was −92 ± 3 mV ($n = 6$) (Fig. 5*C*, right panel). Increasing the external K^+ concentration from 15 to 40 mM shifted E_{rev} to −62 ± 5 mV ($n = 4$) and −30 ± 2 mV ($n = 5$) respectively (*data not shown*). The slope factor between log ($[K^+]_e$) and E_{rev} was estimated by linear regression to be 54 mV, close to the predicted 58 mV value in the Nernst's equation. A Ca^{2+}-free solution abolished both the ACh-induced $[Ca^{2+}]_i$ increase (*see above*) and the K^+ current. Both Ca^{2+} and current oscillations were abolished after obtaining a conventional whole-cell configuration with 10 mM EGTA in the pipette solution. By contrast, a standard pipette solution (no EGTA) had no effect on calcium or basal current levels.

Bath application of atropine (10 nM) (*data not shown*) or 4-DAMP (10 nM) which block muscarinic receptor subtypes abolished both the $[Ca^{2+}]_i$ increase and the K^+ currents (Fig. 6*A*). TEA (20 mM) blocked the ACh-induced $[Ca^{2+}]_i$ increase suggesting that TEA at this concentration acted as a muscarinic receptor antagonist (Fig. 6*B*). Charybdotoxin (ChTx, 10 nM), a known blocker of large conductance Ca^{2+}-dependent K^+ channels (Brau et al., 1990) reversibly reduced the current by 60% in all of the tested cells, but had little effect on Ca^{2+} fluctuations (Fig. 6*C*). Furthermore, quinine (1 mM) totally abolished the ACh-induced potassium current (*data not shown*). It was not possible to determine the effect of quinine on the Ca^{2+} rise because of the autofluoresence exhibited by quinine. Apamin had no effect on the amplitude of the potassium current of the ACh-induced

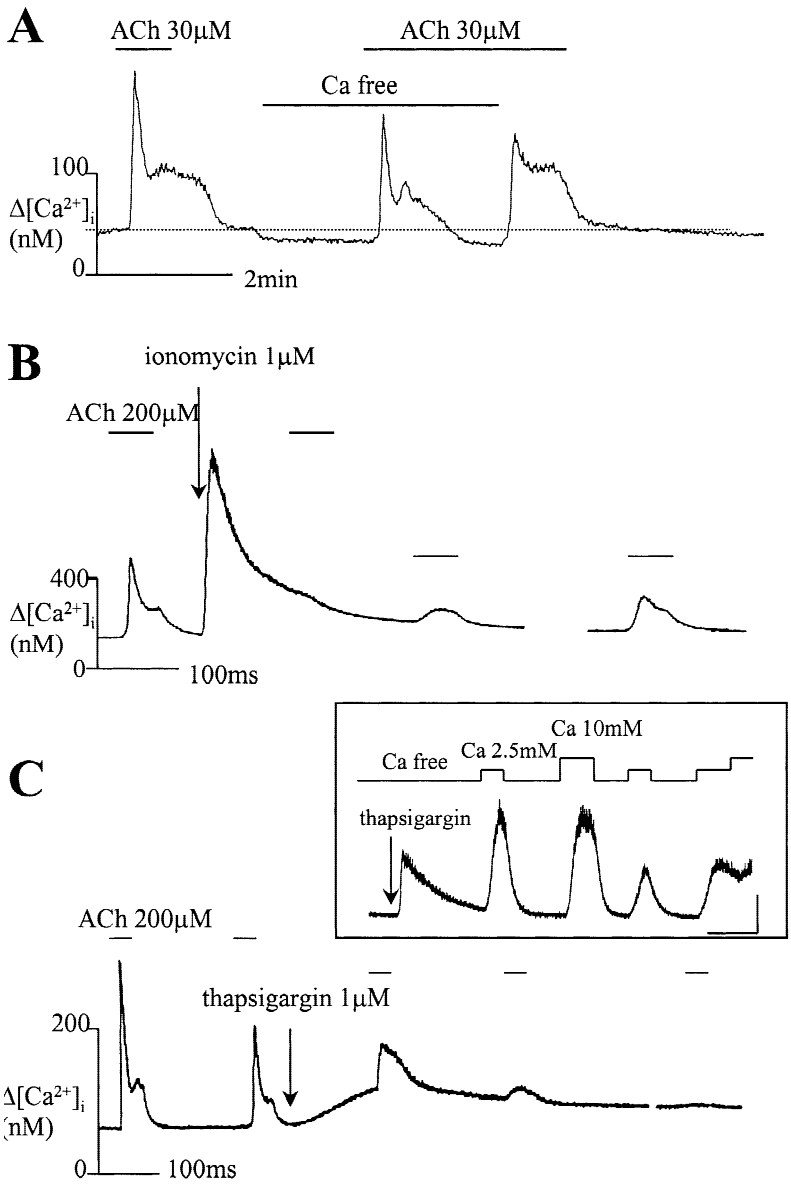

Fig. 4. Calcium origin of the ACh-induced ΔCa. (*A*) ACh (30 μM) bath applied for 1 min increased $[Ca^{2+}]_i$. Removal of external calcium as indicated by the bars resulted in a decrease in basal $[Ca^{2+}]_i$ and in a progressive abolition of the plateau phase induced by ACh. Reintroduction of calcium in the bath made the plateau phase reappear immediately. The dotted line indicates the basal calcium level in 2.5 mM external calcium. (*B*) ACh-induced $[Ca^{2+}]_i$ rise was totally blocked by ionomycin. ACh (200 μM) was pressure-ejected during the time indicated by the bars. Ionomycin (1 μM) was pressure-ejected from a second pipette for 1 sec at the time indicated by the arrow. The inhibition of ACh response was slowly reversible. Interruption in the trace lasted 15 min. (*C*) Thapsigargin pressure ejected for 1 sec (arrow) increased calcium and progressively suppressed the ACh-induced ΔCa. ACh was pressure applied from a second pressure pipette during the time indicated by the bars. In the inset, pressure application of thapsigargin (1 μM) for 1 sec as indicated by the arrow increased calcium in the absence of calcium in the bath. The reintroduction of calcium (as shown by the upper trace) in the bath led immediately to a rise in $[Ca^{2+}]_i$.

$[Ca^{2+}]_i$ increase at concentrations 1 μM or less (*data not shown*).

Discussion

We show that ACh activates muscarinic cholinergic receptors (mAChR) and induces $[Ca^{2+}]_i$ and membrane potential oscillations in a human glioma cell line, U373. These oscillations occur in synchrony and appear to be interdependent. Membrane potential oscillations are caused by the Ca^{2+}-dependent modulation of charybdotoxin-sensitive Ca^{2+}-activated K^+ channels (K_{Ca}). Surprisingly, activation of mACh receptors also inhibited the migration of glioma cells in vitro. Could theses three phenomena be interdependent and could inhibition of cell migration be due to the inhibition of spontaneous $[Ca^{2+}]_i$ oscillations? Mechanism(s) by which oscillations in $[Ca^{2+}]_i$ modulate cell migration are not well understood. However, the phenomenon has previously been observed in other cell systems. For example, the migration of transformed epithelial cell depends on both oscillations in the intracellular Ca^{2+} concentrations ($[Ca^{2+}]_i$) and the polarized activation of a K_{Ca} channel (Schwab et al., 1994; Schwab et al., 1995; Schwab & Oberleithner, 1996; Reinhardt et al., 1998). Verheugen et al. (1997) showed that $[Ca^{2+}]_i$ fluctuations depend primarily on K_{Ca} channel activation in human T lympho-

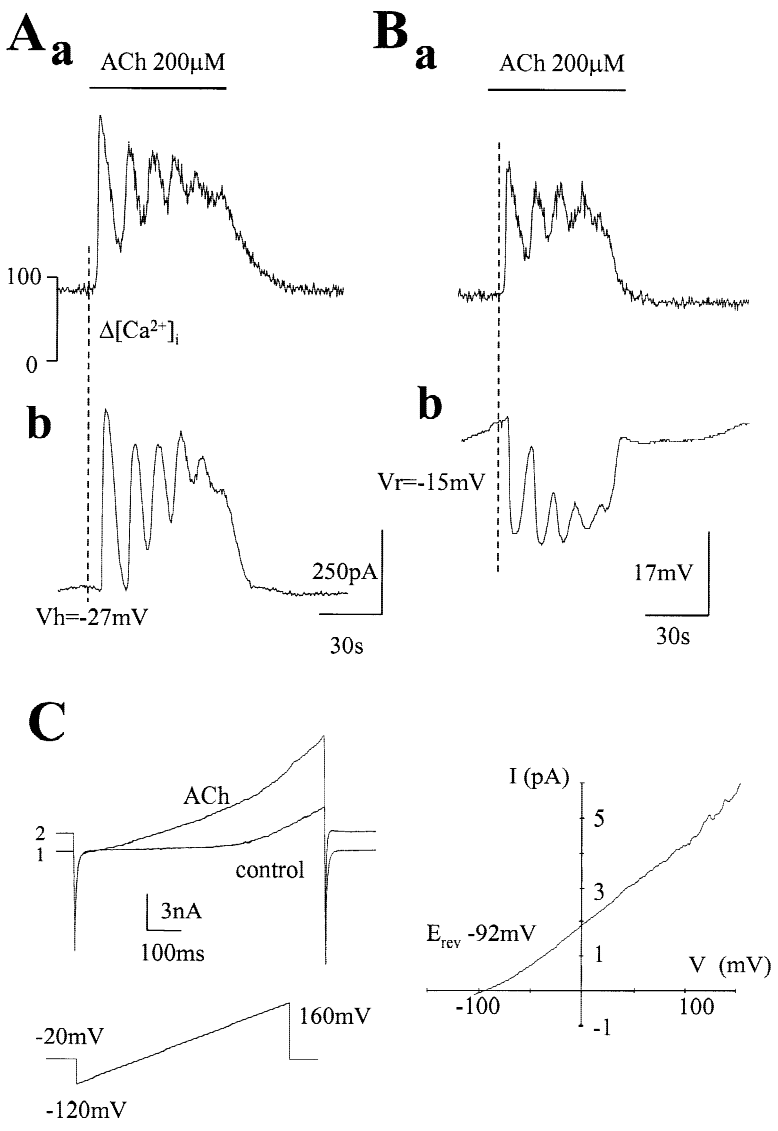

Fig. 5. ACh induces oscillations in calcium, current and membrane potential. (*A*) Under voltage-clamp conditions at a holding potential of −27 mV, ACh (200 μM) induced a simultaneous oscillatory rise in calcium (upper traces) and outward current (lower trace). (*B*) Under current-clamp ACh induced a oscillatory hyperpolarization of the cell (lower trace) in phase with the calcium increase (upper trace). The resting potential was −15 mV. In (*A*) and (*B*), a dashed line was added to show that the calcium increase precedes the change in current or voltage. (*C*) Left panel: current-voltage curve for the ACh-induced current. The current-voltage (*I-V*) relationship for ACh-induced current was determined using voltage ramps (from −120 to +160 mV) as illustrated below the *I-V* curves. Ramp *I-V* curves were recorded before (control) and at the peak of the outward current produced by a 30 sec bath application of ACh (200 μM). The holding potential was −20 mV. Right panel: the reversal potential for the ACh-induced current (E_{rev}) was −92 mV which suggests that ACh induced a potassium current.

cytes. In addition, these oscillations in $[Ca^{2+}]_i$ and K_{Ca} channel activity are consistent with periodic morphological changes during cell migration that could possibly drive cyclic actin polymerization (Ehrengruber, Deranleau & Coates, 1996). While these above studies argue for a role of Ca^{2+} oscillations in cell migration, one of our recent studies (Manning, Parker & Sontheimer, 2000), which is discussed in more detail below, suggests that in glioma cells, cell migration may occur in absence of changes in intracellular Ca^{2+} and suggests that inhibition of cell migration was probably indirectly related to the mitogenic action of muscarine.

Nature of the Receptor Involved in the ACh Response

Our pharmacological studies clearly identified the receptor involved in ACh-induced $[Ca^{2+}]_i$ increases as a muscarinic ACh receptor since muscarine mimicked the ACh response, while the nicotinic agonist DMPP failed to do so. Furthermore, muscarinic antagonists blocked the response. In addition, emptying IP3-sensitive calcium stores with thapsigargin completely abolished the ACh-induced response. These data demonstrate that muscarinic responses in glioma cells are linked to the IP3 pathway as previously reported (Arias-Montano et al., 1994). Among the five cloned and pharmacologically defined muscarinic receptors, three receptors (M1, M3, and M5) are coupled to phospholipase C and phosphoinositide (IP) turnover (Felder, 1995; Loffelholz, 1996; Nahorski, Tobin & Willars, 1997). Since the ACh-induced response is relatively insensitive to pirenzepine (a preferential M1 antagonist at low concentration) and highly sensitive to atropine and 4-DAMP (a preferential M3 antagonist at low concentration), we can exclude the par-

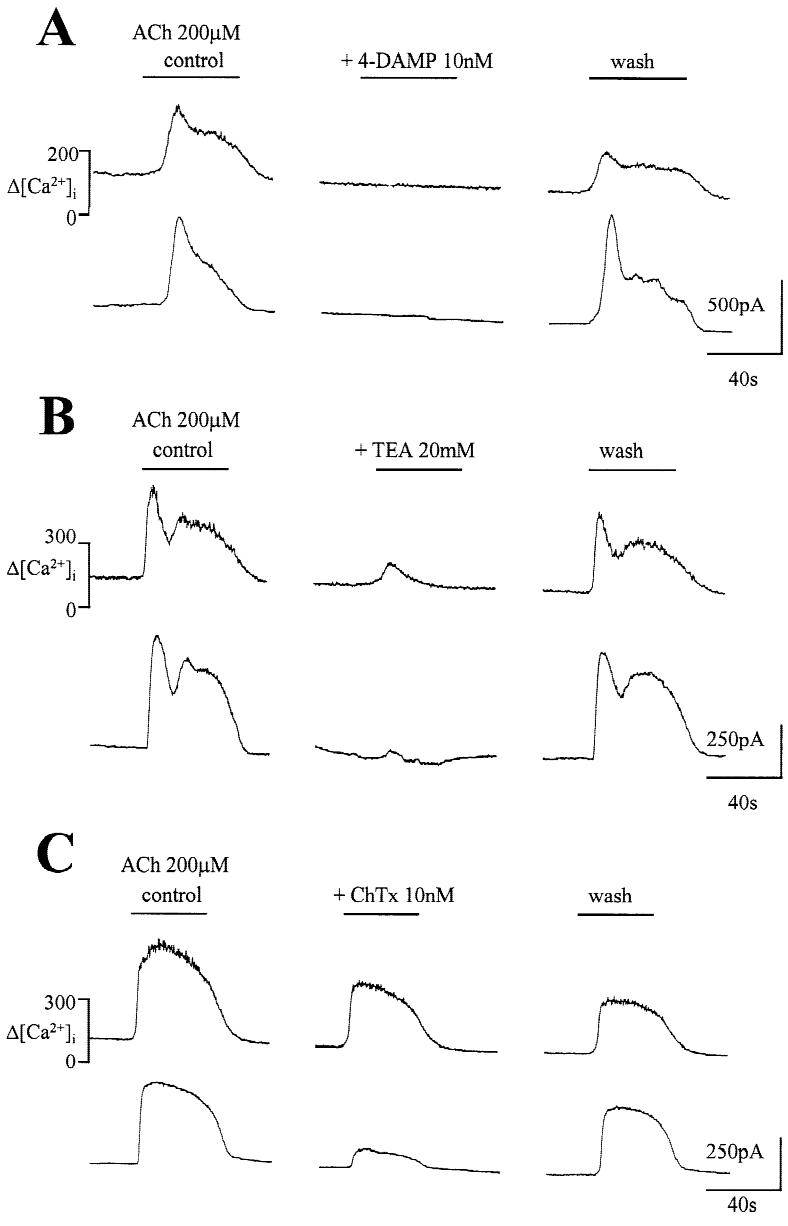

Fig. 6. Pharmacology of the ACh-induced potassium current. Effect of 10 nM 4-DAMP (*A*), 20 mM TEA (*B*) and 10 nM charybdotoxin (*C*) on the ACh-induced ΔCa (upper traces) and outward current (lower traces). For each treatment, data show the effect of ACh before (control, left panel) during (drug, middle panel) and after the wash out (wash, right panel) of the drug. ACh (200 μM) was bath applied during the time indicated by the bar. Cells were voltage-clamped at −20 mV. The interval between the application of ACh was 3 min except for the wash out of 4-DAMP which took 6 min.

ticipation of M1 receptors in the ACh-mediated response. In addition, Arios-Montano et al. (1994) demonstrated that stimulation of IP turnover in U373 cells was mediated by the M3 subtype mAChR. We therefore suggest that the ACh effects on internal Ca^{2+} and membrane currents were a result of activation of muscarinic receptors of the M3 subtype.

Muscarinic Receptor Activated Calcium Influx

ACh induced a biphasic increase in calcium. The first transient phase resulted from a mobilization of calcium from internal stores since this first phase remained in the absence of external Ca^{2+}. This transient phase was inhibited by TG, an inhibitor of the Ca-ATPase pump responsible for sequestering Ca^{2+} into IP3-sensitive stores (Inesi & Sagara, 1994). As we show in Fig. 4C, TG induced an intracellular calcium increase, and during this increase ACh-induced $[Ca^{2+}]_i$ changes were reduced and then suppressed because of the inability of the endoplasmic reticulum to refill. In addition, TG increased the basal Ca^{2+} level by apparently stimulating an influx of Ca^{2+} through the plasma membrane (inset in Fig. 4*C*). This mechanism of Ca^{2+} entry called capacitive entry has been observed in various nonexcitable cells and is believed to be involved in the refilling of calcium stores through activation of calcium release-activated channels

(Penner, Fasolato & Hoth, 1993). This implies that both IP3-mediated intracellular calcium increase and capacitive calcium influx coexist in U373 astrocytoma cells. We therefore suggest that ACh-induced biphasic Ca^{2+} rise is mediated by IP3-sensitive calcium release (transient phase) that might lead to activation of capacitive calcium entry (plateau).

Mechanisms of Calcium and Membrane Potential Oscillations

Our data represent the first description of correlated Ca^{2+} and membrane potential oscillations in glioma cells in response to mAChR activation. Similar oscillations have been observed in astrocytes stimulated by excitatory amino acids (Charles et al., 1991; Jensen & Chiu, 1990), leading to several proposed models (Fewtrell, 1993; Finkbeiner, 1993). One model is based on the existence of oscillations in IP3 levels and includes a one pool model where IP3 is regulated by Ca^{2+} concentration. The second model, which does not propose fluctuations in IP3, includes a two pool compartment composed of an IP3-sensitive and a Ca^{2+}-sensitive (commonly called calcium-induced calcium release) store. We can exclude the two pool model in U373 cells since these cells are insensitive to caffeine and ryanodine. It has also been proposed that membrane potential fluctuations might participate in calcium oscillations. Changes in membrane potential that might participate in the generation of Ca^{2+} oscillations include depolarization and a subsequent opening of voltage-dependent Ca^{2+} channels, and/or hyperpolarization resulting in an increase in the inward driving force for Ca^{2+}. We did not detect the presence of any inward K^+, Na^+ or voltage-dependent Ca^{2+} currents. The absence of inwardly rectifying potassium channels could explain the low resting potential (−27 mV) of U373 cells in our study, similar to the low resting potential of neoplastic cells (Bordey & Sontheimer, 1998). Activation of mAChR-induced oscillations of K_{Ca} channels could determine the membrane potential over a large range since K_{Ca} currents exhibit a high sensitivity to calcium. However, these currents did not induce Ca^{2+} oscillations since these oscillations are still present when recordings were obtained under voltage-clamp conditions with constant driving force for Ca^{2+} entry. Thus it is more likely that IP3 induces these Ca^{2+} oscillations.

Migration and K_{Ca} Channels: Suppression by mAChR Activation

Oscillating activity of K_{Ca} channels are required for the migration of transformed epithelial cells (Schwab et al., 1994; Schwab & Oberleithner, 1996). In glioma cells, activation of mAChR induced oscillations in membrane potentials presumably due to opening of K_{Ca} channels. One would have expected that muscarine or acetylcholine may induced cell migration. However, in our experiments, muscarine inhibited migration. How may this discrepancy come about? We suggest that these effects are indirect rather than direct and more specifically relate to the well documented mitogenic action of muscarine on glioma cells (Guizetti et al., 1997).

Specifically, we recently found in a related study that lysophosphatidic acid (LPA), a serum borne signaling molecule, induces similar Ca^{2+} oscillations in glioma cells by activating Ca^{2+} release from intracellular stores. These Ca^{2+} signals involve activation of phospholipase C. LPA also acted as a potent chemokine, and induced chemotactic migration of glioma cells. However, migration continued undisturbed even if intracellular Ca^{2+} fluctuations were completely inhibited using the phospholipase C inhibitor U73122 (Manning et al., 2000). Taken together with findings in the present study, these findings argue that parallel signalling pathways mediate changes in BK-current activity and cell migration.

We like to speculate that muscarine inhibition of glioma cell migration is an indirect effect. It has been shown that activation of ACh receptors potently stimulates glioma cell proliferation (Guizetti et al., 1997). Moreover, BK activation has been linked to enhanced cell-cycle activity in a number of cell types including tumor cells (Liu et al., 1998; Vaur et al., 1998; Wiecha et al., 1998) and we were able to inhibit glioma growth using BK antagonists such as iberiotoxin (*unpublished results*). An interdependence between BK activity and cell growth thus seems highly likely. A widely held theory dubbed “go-or-grow” (Berens, Rutka & Rosenblum, 1990; Merzak et al., 1994; Koochekpour, Merzak & Pilkington, 1995; Chicoine & Silbergeld, 1997) suggests that cells either divide (grow) or migrate (go) but do not do both at the same time. We thus suggest that the growth stimulatory effect of muscarine would indirectly inhibit migration as it potently stimulates growth. Whether the time frame with which we observed these effects is consistent with that explanation remains to be shown. Clearly, further studies are necessary to further elucidate the biology underlying muscarine actions on glioma migration. The responsiveness of glioma cells to ACh receptor activation and its enhanced presence in the cerebrospinal fluid of glioma patients suggests an important role of ACh signalling in glioma biology.

This work was supported by CNRS, University Louis Pasteur, Direction des Recherches et Techniques (DRET-91-13 1), INSERM (CRE 9006-1 1), and National Institutes of Health grants RO1-NS31234 and RO1-NS36692.

References

Arias-Montano, J.A., Berger, V., Young, J.M. 1994. Calcium-dependence of histamine- and carbachol-induced inositol phosphate

formation in human U373 MG astrocytoma cells: comparison with HeLa cells and brain slices. *Br. J. Pharmacol.* **111:**598–608

Berens, M.E., Rutka, J.T., Rosenblum, M.L. 1990. Brain tumor epidemiology, growth, and invasion. *Neurosurg. Clin. N. Am.* **1:**1–18

Bordey, A., Sontheimer, H. 1998. Electrophysiological properties of human astrocytic tumor cells in situ: enigma of spiking astrocytes. *J. Neurophysiol.* **79:**2782–2793

Brau, M.E., Dreyer, F., Jonas, P., Repp, H., Vogel, W. 1990. A K^+ channel in *xenopus* nerve fibers selectively blocked by bee and snake toxins: binding and voltage-clamp experiments. *J. Physiol.* **420:**365–385

Brismar, T. 1995. Physiology of transformed glial cells. *Glia* **15:**231–243

Bychkovskii, V.N., Pleshtis, S.A., Sobeshchanskii, G.V. 1998. Neurohumoral shifts in brain tumor patients. *Zhurnal Voprosy Neirokhirurgii Imeni N - N - Burdenko* **6:**27–30

Charles, A.C., Merill, J.E., Dirksen, E.R., Sanderson, M.J. 1991. Intercellular signaling in glial cells: calcium waves and oscillations in response to mechanical stimulation and glutamate. *Neuron* **6:**983–992

Chicoine, M.R., Silbergeld, D.L. 1997. Mitogens as motogens. *J. Neurooncol.* **35:**249–257

Ehrengruber, M.U., Deranleau, D.A., Coates, T.D. 1996. Shape oscillations of human neutropil leukocytes: characterization and relationship to cell motility. *J. Exp. Biol.* **199:**741–747

Felder, C.C. 1995. Muscarinic acetylcholine receptors: signal transduction through multiple effectors. *FASEB J.* **9:**619–625

Feldkamp, M.M., Lau, N., Guha, A. 1997. Signal transduction pathways and their relevance in human astrocytomas. *J. Neurooncol.* **35:**223–248

Fewtrell, C. 1993. Ca^{2+} oscillations in non-excitable cells. *Annu. Rev. Physiol.* **55:**427–454

Finkbeiner, S.M. 1993. Glial calcium. *Glia* **9:**83–104

Gomez, T., Snow, D., Letourneau, P. 1995. Characterization of spontaneous calcium transients in nerve growth cones and their effect on growth cone migration. *Neuron* **14:**1233–1246

Grynkiewicz, G., Poenie, M., Tsien, R.Y. 1985. A new generation of Ca^{2+} indicators with greatly improved fluorescence properties. *J. Biol. Chem.* **260:**3440–3450

Guha, A. 1998. Ras activation in astrocytomas and neurofibromas. *Can. J. Neurol. Sci.* **25:**267–281

Guizetti, M., Costa, P., Peters, J., Costa, L.G. 1997. Acetylcholine as a mitogen: muscarinic receptor-mediated proliferation of rat astrocytes and human astrocytoma cells. *Eur. J. Pharmacol.* **297:**265–273

Hamill, O.P., Marty, A., Neher, E., Sakmann, B., Sigworth, F.J. 1981. Improved patch-clamp techniques for high-resolution current recording from cells and cell-free membrane patches. *Pfluegers Arch.* **391:**85–100

Inesi, G., Sagara, Y. 1994. Specific inhibitors of intracellular Ca^{2+} transport ATPases. *J. Membrane Biol.* **141:**1–6

Jensen, A.M., Chiu, S.Y. 1990. Fluorescence measurements of changes in intracellular calcium induced by excitatory amino acids in cultured cortical astrocytes. *J. Neurosci.* **10:**1165–1175

Komuro, H., Rakic, P. 1996. Intracellular Ca^{2+} fluctuations modulate the rate of neuronal migration. *Neuron* **17:**275–285

Koochekpour, S., Merzak, A., Pilkington, G.J. 1995. Extracellular matrix proteins inhibit proliferation, upregulate migration and induce morphological changes in human glioma cell lines. *Eur. J. Cancer* **31A:**375–380

Liu, S.I., Chi, C.W., Lui, W.Y., Mok, K.T., Wu, C.W., Wu, S.N. 1998. Correlation of hepatocyte growth factor-induced proliferation and calcium-activated potassium current in human gastric cancer cells. *Biochim. Biophys. Acta* **1368:**256–266

Loffelholz, K. 1996. Muscarinic receptors and cell signalling. *Prog. Brain Res.* **109:**191–194

Manning, T.J., Jr., Parker, J.C., Sontheimer, H. 2000. Role of lysophosphatidic acid and Rho in glioma cell motility. *Cell Motil. Cytoskeleton* **45:**185–199

Marks, P.W., Maxfield, F.R. 1990. Transient increases in cytosolic free calcium appear to be required for the migration of adherent human neutrophils. *J. Cell Biol.* **110:**43–52

Merzak, A., McCrea, S., Koocheckpour, S., Pilkington, G.J. 1994. Control of human glioma cell growth, migration and invasion in vitro by transforming growth factor beta 1. *Br. J. Cancer* **70:**199–203

Nahorski, S.R., Tobin, A.B., Willars, G.B. 1997. Muscarinic M_3 receptor coupling and regulation. *Life Sci.* **60:**1039–1045

Penner, R., Fasolato, C., Hoth, M. 1993. Calcium influx and its control by calcium release. *Curr. Opin. Neurobiol.* **3:**368–374

Rae, J., Cooper, K., Gates, P., Watsky, M. 1991. Low access resistance perforated patch recordings using amphotericin B. *J. Neurosci. Methods* **37:**15–26

Rakic, P., Komuro, H. 1994. The role of receptor/channel activity in neuronal cell migration. *J. Neurobiol.* **26:**299–315

Reinhardt, J., Golenhofen, N., Pongs, O., Oberleithner, H., Schwab, A. 1998. Migrating transformed MDCK cells are able to structurally polarize a voltage-activated K^+ channel. *Proc. Natl. Acad. Sci.* **95:**5378–5382

Schwab, A., Finsterwalder, F., Kersting, U., Danker, T., Oberleithner, H. 1997. Intracellular Ca^{2+} distribution in migrating transformed epithelial cells. *Pfluegers Arch.* **434:**70–76

Schwab, A., Gabriel, K., Finsterwalder, F., Folprecht, G., Greger, R., Kramer, A., Oberleithner, H. 1995. Polarized ion transport during migration of transformed Madin-Darby canine kidney cells. *Pfluegers Arch.* **430:**802–807

Schwab, A., Oberleithner, H. 1996. Plasticity of renal epithelial cells: the way a potassium channel supports migration. *Pfluegers Arch.* **432:**87–93

Schwab, A., Wojnowski, L., Gabriel, K., Oberleithner, H. 1994. Oscillating activity of a Ca^{2+}-sensitive K^+ channel. *J. Clin. Invest.* **93:**1631–1636

Shapiro, W.R., Shapiro, J.R. 1998. Biology and treatment of malignant glioma. *Oncology* **12:**233–240

Vaur, S., Bresson-Bepoldin, L., Dufy, B., Tuffet, S., Dufy-Barbe, L. 1998. Potassium channel inhibition reduces cell proliferation in the GH3 pituitary cell line. *J. Cell Physiol.* **177:**402–410

Verheugen, J.A.H., Le Deist, F., Devignot, V., Korn, H. 1997. Enhancement of calcium signaling and proliferation responses in activated human T lymphocytes. *Cell Calcium* **21:**1–17

Wiecha, J., Munz, B., Wu, Y., Noll, T., Tillmanns, H., Waldecker, B. 1998. Blockade of Ca^{2+}-activated K^+ channels inhibits proliferation of human endothelial cells induced by basic fibroblast growth factor. *J. Vasc. Res.* **35:**363–371